Biochemistry and Biophysics Reports 41 (2025) 101935

Contents lists available at ScienceDirect

Biochemistry and Biophysics Reports

journal homepage: www.elsevier.com/locate/bbrep

Comprehensive analysis of differential mRNA and circRNA profiles in primary and metastatic pancreatic neuroendocrine tumors

Gang Li [a,1], Jing Zhang [b,1], Bentuo Zhang [c], Dan Wang [c], Zequn Wang [c], Yan Pan [c,**], Lijie Ma [b,*]

[a] Department of General Surgery, Peking University Third Hospital, Beijing, 100191, China
[b] Inner Mongolia Key Laboratory of Molecular Biology, Inner Mongolia Medical University, Hohhot, 010059, China
[c] Department of Pharmacology, School of Basic Medical Sciences, Health Science Center, Peking University, Beijing, 100191, China

ARTICLE INFO

Keywords:
Primary pancreatic neuroendocrine tumor
Live metastasis
RNA sequencing
CircRNA microarrays
Tumor adhesion

ABSTRACT

The diagnosis of primary pancreatic neuroendocrine tumors (pNETs) presents significant challenges, and metastatic pancreatic neuroendocrine tumors are associated with high mortality. Understanding the characteristics of these tumors, particularly the key molecules involved in metastasis, is essential. To address this, we utilized mRNA expression data from human pNET and metastatic pancreatic tumor tissues available in the GEO database and integrated this data with bioinformatics analyses. And then we collected clinical primary tumor and liver metastasis samples from patients with pNETs, we conducted a comprehensive analysis of circular RNAs (circRNAs) to identify key circRNAs associated with the onset and metastasis of pNETs. We found that in pNET development and metastasis, 11 genes and 14 circRNAs were notably upregulated, while 25 genes and 35 circRNAs were significantly downregulated, compared to nearby non-cancerous tissue. Our analysis of differentially expressed RNA and circRNA genes revealed that tumor cell adhesion and integrin activation, regulated by genes like PIEZO1, IFT74, SKAP1, GPX1, F7, VTN, and OMG, are strongly linked to pNET metastasis. We found that SKAP1 levels are positively associated with tumor progression in pNET patients. Overall, our research indicates that the SKAP1-mediated pathway is crucial in pNET development and metastasis.

1. Introduction

Pancreatic neuroendocrine tumors (pNETs) are rare tumors arising from neuroendocrine cells, with increasing incidence and prevalence. They develop from either abnormal growth of endocrine pancreatic cells or pluripotent exocrine pancreatic cells [1]. Pancreatic neuroendocrine tumors can be categorized into functional and non-functional types based on their hormone secretion capabilities [2]. Functional pNETs can be diagnosed earlier due to their hormone symptoms [3]. Non-functional pNETs, accounting for 60%–90 % of all cases, are frequently asymptomatic and often go undiagnosed until they are advanced and inoperable, leading to poorer outcomes for patients [4]. Identifying additional biomarkers and molecules is crucial for diagnosing and treating metastasis pNETs. Understanding the genomic changes and mechanisms behind this non-functional pNET's pathogenesis is essential to discover new diagnostic targets.

Drug therapies for advanced, unresectable, or metastatic pNETs include somatostatin analogs (octreotide, lanreotide), mTOR inhibitor (everolimus), tyrosine kinase inhibitor (sunitinib), chemotherapeutics (5-fluorouracil, streptozotocin, capecitabine, temozolomide), and peptide receptor radionuclide therapy. However, malignant tumor progression and resistance hinder pNET treatment [5]. We need to grasp the molecular mechanisms behind pNET pathogenesis and metastasis to guide drug therapy development.

Some molecular profiling studies have identified key pNET-signature genes, such as MEN1, ATRX/DAXX, and p53, and pathways like mTOR, INK4A/ARF, RB1, VHL, NF1, RAS-RAF-MEK-ERK, and somatostatin receptor signaling. Despite this, the main molecular changes in pNET development and progression remain unclear due to its complexity.

Transcriptome research investigates gene function and uncovers biological processes and molecular mechanisms in diseases. RNA sequencing is commonly used to analyze differentially expressed genes

* Corresponding author.
** Corresponding author.
E-mail addresses: pannay26@hsc.pku.edu.cn (Y. Pan), nmmalj@hotmail.com (L. Ma).
[1] They are co-first authors.

https://doi.org/10.1016/j.bbrep.2025.101935
Received 10 August 2024; Received in revised form 17 January 2025; Accepted 22 January 2025

in these conditions [6]. Circular RNA (circRNA) is a novel RNA type with a closed-loop structure, distinct from linear RNA, and is abundant in eukaryotic transcriptomes [7]. Most circular RNAs consist of conserved exon sequences across species and exhibit tissue and developmental stage-specific expression. Their resistance to nucleases makes them more stable than linear RNAs, offering clear benefits for developing new clinical diagnostic markers [8]. Recent studies indicate that circular RNA can regulate target gene expression by acting as competitive endogenous RNA (ceRNA) or by binding with RNA binding proteins (RBPs) [9].

In this study, we employed RNA transcriptome and circRNA profiling with bioinformatics to explore the mechanisms behind tumor development in non-functional pNETs, aiming to identify key molecules and pathways for predicting metastasis and aiding diagnosis. These findings could potentially guide clinical detection and treatment of pNET malignancy or metastasis.

2. Materials and methods

2.1. Tumor specimens obtained from individuals diagnosed with pNET

During surgery, samples of primary carcinoma tumor tissue, liver metastasis, and tissues adjacent to cancer were collected from pNET patients. Samples were excluded if patients had received chemotherapy or radiation, had other malignant tumors, immune system diseases, or blood system infections. Patients aged 36–70, regardless of gender, with normal blood pressure and clinically diagnosed with stage 2 or higher pNET, showing 10%–40% Ki67 positive were included. A 5 mm × 5 mm lung cancer area was analyzed. The study received approval from the Peking University Third Hospital Medical Science Research Ethics Committee, and all patients provided written informed consent prior to tissue sample collection.

2.2. pNET sample data from the GEO database and differential mRNA analysis via RNA sequencing

In this study, we utilized the NCBI GEO database to identify potential functional genes involved in pNETs tumorigenesis and metastasis by screening for differentially expressed genes (DEGs). Using GPL20945 18.5K human oligo microarrays from Ohio State University's cancer center, as part of the GSE73338 database, we analyzed global gene expression in pancreatic endocrine tumors. It included 96 samples: 63 non-functional pNETs, 17 insulinomas, 5 normal pancreas, 4 normal pancreas islets, and 7 metastases. Our study analyzed 63 non-functional pNETs, 9 normal tissues, and 7 metastasis samples, categorized as Tumor, Normal, and Metastases groups. We used GEO2R for differential analysis to identify DEGs linked to pNET tumorigenesis and metastasis, with thresholds of $|\mathrm{Log_2FoldChange}| > 1$ and p-value <0.05.

2.3. CircRNA differential expression analyses

We used the Human circular RNA array V2.0 from ArrayStar, covering 13,617 human circRNAs, and analyzed by Kang Chen Bio-tech. No laser microdissection or whole tissue harvesting from pancreatic islet cells was done before RNA isolation. Total RNA was extracted from primary tumor tissues, liver metastases, and adjacent tissues using TRIzol reagent. Linear RNAs were removed from total RNAs using RNase R to enrich circular RNAs, which were then amplified and transcribed into fluorescent cRNA with a random priming technique (Arraystar Super RNA Labeling Kit; Arraystar). Labeled cRNAs were purified using the RNeasy Mini Kit (QIAGEN), and their concentrations and specific activities were assessed with a NanoDrop ND-1000. One microgram of each labeled cRNA was fragmented by adding 5 μL of 10 × blocking agent and 1 μL of 25 × fragmentation buffer, heating at 60 °C for 30 min, and then diluting with 25 μL of 2 × hybridization buffer. A 50 μL hybridization solution was added to a gasket slide and combined with a circRNA microarray slide. The slides were incubated for 17 h at 65 °C in an Agilent oven, then washed, fixed, and scanned with an Agilent G2505C scanner. Images were analyzed using Agilent feature extraction software. Data normalization and processing were conducted with the R software package [10]. After quantile normalization of the raw data, low-intensity filtering was performed.

2.4. Functional enrichment analysis

GO and KEGG pathway enrichment analyses were conducted using the "org.Hs.eg.db" and "clusterProfiler" R package [10]s. Gene identifiers were converted to H. sapiens Entrez IDs, and enrichment was performed using KEGG and GO against the entire genome as the background. P-values were calculated, and significant differences were identified using the Benjamini-Hochberg method, with p-values <0.05 deemed statistically significant.

2.5. Protein-protein interaction (PPI) network construction

The STRING database (https://string-db.org/) predicts protein-protein interactions (PPI) to create a PPI network. DEGs were input into STRING, using a PPI interaction score >0.4 as the threshold. Cytoscape visualized the network, and Centiscape 2.2 identified hub genes by calculating network centralities.

2.6. Construction of CeRNA network

The ceRNA network was built using the miRcode database to identify circRNA-miRNA interactions and matched miRNA interactions. miRNA-targeted mRNAs were predicted using miRTarBase, miRDB, and TargetScan databases. Only mRNAs found in all three databases and overlapping with the mRNAs were included in the network, which was visualized with Cytoscape [11].

2.7. Reverse transcription quantitative polymerase chain reaction (RT-qPCR)

Total RNA was isolated from clinical samples utilizing the TRIzol reagent (Invitrogen, California, USA) following the manufacturer's protocol. Complementary DNA (cDNA) synthesis was conducted using the cDNA First Strand Synthesis Kit (Abclonal, Wuhan, China). Reverse transcription quantitative polymerase chain reaction (RT-qPCR) was carried out in accordance with the SYBR Green Fast qPCR Mix (Mei5bio, Beijing, China) guidelines, under the following thermal cycling conditions: initial denaturation at 95 °C for 30s, then 45cycles including 95 °C for 5s and 60 °C for 30s for annealing and elongation. The relative expression of target genes was normalized to GAPDH and quantified with $2^{-\Delta\Delta Ct}$ method. The oligonucleotide primer sequences used are shown in Table 1.

2.8. Western blotting

Tumor cell lysates were prepared with RIPA buffer containing protease inhibitors, and protein concentration was measured using the BCA method. Proteins were separated by SDS-PAGE and transferred to PVDF membranes, which were blocked with 5 % milk for 40 min at room temperature. Membranes were incubated overnight at 4 °C with primary antibodies, followed by a 1-h incubation with secondary antibodies at room temperature. Visualization was done using the ECL system, and ImageJ (Version 1.53e) was used for analyzing immunoblot band intensities.

2.9. Statistical analysis

Data are presented as mean ± SD. The correlation was evaluated by Spearman's correlation analysis. Student's t-test was used to compare

Table 1
The oligonucleotide primer sequences of circRNAs.

Gene name	Primer sequence
GAPDH	F:5′GGGAAACTGTGGCGTGAT 3′ R:5′GAGTGGGTGTCGCTGTTGA 3′
hsa_circ_0012779	F:5′ACACCAAGCGACACGAGTTATT 3′ R:5′ TTGTAGGATCTAAAGGGTCCATG 3′
hsa_circ_0004365	F:5′ TTGATTGTTCGTATTGGCACTG 3′ R:5′ TTCACGTTGGGGTTGAAAGAG 3′
hsa_circ_0087104	F:5′ GGCTGTGCTCATTGATTCAGG 3′ R:5′ AAAATAAACCACCTCAGATTCTCC 3′
PIEZO1	F: 5′ CATAGGGGTCACAAGGCTGG 3′ R: 5′ GAGGAGACCACCAAGATGCC 3′
F7	F: 5′ CTCAGGAGGAGAAACACGGG 3′ R: 5′ CCAGAACAGCTTCGTCCTCT 3′
IFT74	F: 5′ AGCAAGACCAGGTTCTCGTG 3′ R: 5′ ATTTGCCTCTGGGGACCTTT 3′
SKAP1	F: 5′ GCACTCGACGAAAAGGAGACTA 3′ R: 5′ GGAACAATCCCAACGAGGCT 3′
GPX1	F: 5′ CCAGTTTGGGCATCAGGAGA 3′ R: 5′ AGCATGAAGTTGGGCTCGAA 3′
VTN	F: 5′ GTGCAAGCCCCAAGTGACTC 3′ R: 5′ CCTCGCCATCGTCATAGACC 3′
OMG	F: 5′ GCCTCAACAAAGCACAACCC 3′ R: 5′ AGCCAGCATGACCACAACAT 3′

the difference between two groups, and the ANOVA test was used to compare the difference between more than two groups by using GraphPad Prism 8.0 software. Results were statistically significant at $p < 0.05$. Significance levels: $*p < 0.05$; $**p < 0.01$; $***p < 0.001$; $****p < 0.0001$; ns indicates no significance.

3. Results

3.1. Differential gene analysis of pNET tissue from the GEO database

We analyzed data from 63 primary tumor tissues, 7 liver metastasis sites, and 9 cancer-adjacent tissues (5 pancreatic and 4 islet) using GEO2R. Comparing these, we identified 11 up-regulated and 25 down-regulated genes across adjacent tissues, tumors, and metastases (Fig. 1, Table 2). These gene changes are more pronounced in liver metastases (M) than in primary tumors (T) compared to adjacent tissues (N).

3.2. Differential gene-associated GO and KEGG pathways

The analysis of significantly up-regulated and down-regulated genes was conducted using org.Hs.eg.db and cluster Profiler R packages. GO analysis covered biological processes (BP), cell components (CC), and molecular functions (MF). For GO and KEGG enrichment, 11 up-regulated and 25 down-regulated genes were examined, applying the BH p-value correction method. Fig. 2 lists the top 5 altered GO (BP, CC, MF) and KEGG pathways. Up-regulated genes were notably involved in processes like positive regulation of wound healing and leukocyte adhesion. The cell components were enriched in peptidase inhibitor and serine-type peptidase complexes, as well as collagen-containing extracellular matrix. The molecular function showed enrichment in toxic substance binding, SUMO ligase activity, and high-density lipoprotein particle binding (Fig. 2A). Down-regulated genes were enriched in digestion, lipid catabolism, and antimicrobial response. The cell

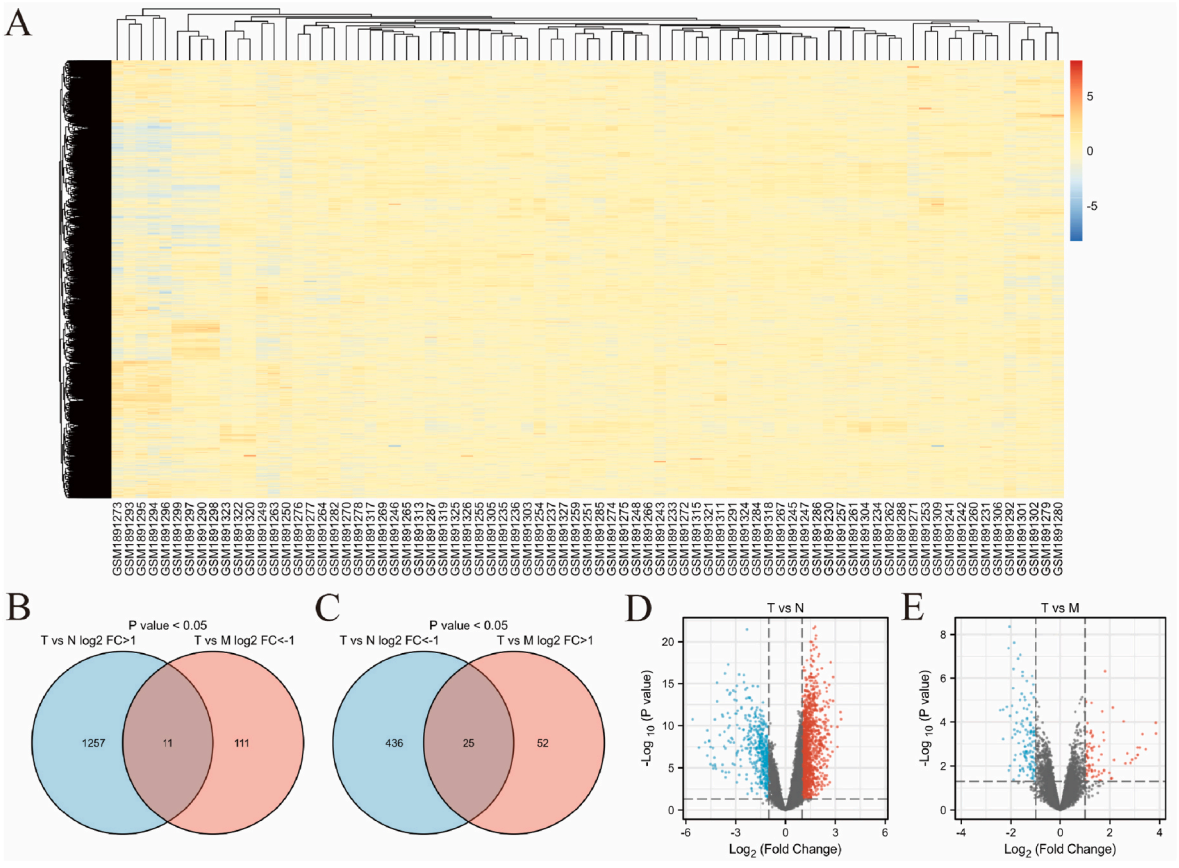

Fig. 1. Analysis of Differential Genes in pNET Tissues from GEO Database A. Differential genes identified among pNET primary tumors (T), liver metastases (M), and adjacent non-cancerous tissues (N) using GEO data. B. Eleven genes were progressively up-regulated from adjacent tissues to primary tumors and liver metastases. C. Twenty-five genes were progressively down-regulated from adjacent tissues to primary tumors and liver metastases. D. Volcano plot comparing gene differences between T and N groups. E. Volcano plot comparing gene differences between T and M groups. Significance was determined with n = 3 and $p < 0.05$.

Table 2
The 11 up-regulated and 25 down-regulated genes successively in the adjacent tissues, primary tumor tissues and liver metastatic foci of pNET.

	No	Gene Name	T vs N		T vs M	
			LogFC	P value	LogFC	P value
Up-regulated	1	C9orf45	1.3339886	2.93 × 10-5	−1.6326277	2.89 × 10-4
	2	EEF1A2	1.0846413	7.63×10^{-4}	−1.0531902	4.47×10^{-3}
	3	F7	1.237987	1.27×10^{-3}	−1.0736549	1.62×10^{-2}
	4	GUCY2C	1.9789791	1.24×10^{-2}	−1.8963779	4.16×10^{-2}
	5	HSPD1	1.0242141	5.10×10^{-3}	−1.2189876	8.61×10^{-3}
	6	LAG3	1.2304037	8.15×10^{-3}	−1.0471607	4.84×10^{-2}
	7	LY6H	1.0684171	2.15×10^{-2}	−1.1153678	3.71×10^{-2}
	8	PIAS4	1.0186764	4.98×10^{-7}	−1.1006764	1.97×10^{-6}
	9	SKAP1	1.0816928	4.80×10^{-2}	−1.6382554	1.49×10^{-2}
	10	ST6GALNAC5	1.2078811	1.35×10^{-2}	−1.6081817	2.85×10^{-3}
	11	VTN	1.1089399	2.92×10^{-2}	−1.3358856	2.61×10^{-2}
Down-regulated	12	AMY2A	−2.7871589	6.83×10^{-5}	2.1717065	5.30×10^{-3}
	13	BCAT1	−2.3199031	3.34×10^{-22}	1.1448505	9.72×10^{-3}
	14	C10orf116	−1.0287897	2.19×10^{-8}	1.2173243	3.20×10^{-4}
	15	CAPNS1	−3.6980764	2.90×10^{-8}	1.5467251	2.48×10^{-2}
	16	CELA3B	−3.6177832	1.33×10^{-4}	3.8553884	3.31×10^{-4}
	17	CLPS	−4.1893238	1.32×10^{-5}	3.1252922	3.14×10^{-3}
	18	CPA1	−4.3860958	5.28×10^{-6}	3.1114913	3.14×10^{-3}
	19	CPA2	−4.5221327	3.68×10^{-6}	3.033609	4.36×10^{-3}
	20	CPB1	−2.9249809	5.29×10^{-4}	3.8459963	1.07×10^{-4}
	21	CTRB1	−3.1836188	3.23×10^{-6}	1.7628788	1.67×10^{-2}
	22	CTRC	−3.81186	2.50×10^{-5}	3.1988445	1.45×10^{-3}
	23	GCG	−2.2852224	1.23×10^{-2}	2.8322934	7.21×10^{-3}
	24	IAPP	−3.7713445	8.21×10^{-12}	1.279442	1.77×10^{-2}
	25	INS	−3.5969247	3.40×10^{-5}	3.1107405	1.44×10^{-3}
	26	NUPR1	−4.5165452	3.38×10^{-8}	1.982596	2.04×10^{-2}
	27	PLA2G1B	−3.403989	3.27×10^{-5}	3.3125465	3.52×10^{-4}
	28	PLCB1	−3.1110278	9.83×10^{-9}	1.2606659	1.46×10^{-2}
	29	PLCE1	−3.2546993	2.94×10^{-9}	1.5465877	5.34×10^{-3}
	30	PNLIP	−4.3510027	1.22×10^{-5}	3.4405054	1.73×10^{-3}
	31	PNLIPRP1	−5.6025843	1.77×10^{-11}	1.6377979	4.57×10^{-2}
	32	PNLIPRP2	−5.2123863	3.95×10^{-8}	2.0528723	3.69×10^{-2}
	33	PRSS1	−3.7962788	4.26×10^{-6}	2.7030211	2.67×10^{-3}
	34	PRSS2	−4.2384456	6.81×10^{-6}	2.8910213	5.08×10^{-3}
	35	REG1B	−4.7076512	3.43×10^{-7}	2.6271831	7.56×10^{-3}
	36	REG3A	−4.2548799	4.13×10^{-6}	2.0814471	3.56×10^{-2}

component was enriched in secretory granule, cytoplasmic vesicle, and vesicle lumens. The molecular function was enriched in lipase activity, serine-type endopeptidase activity, and triglyceride lipase activity (Fig. 2B).

The KEGG analysis showed that up-regulated genes were enriched in legionellosis, complement and coagulation cascades, and glycosphingolipid biosynthesis (Fig. 2C), while down-regulated genes were enriched in pancreatic secretion, protein digestion and absorption, and fat digestion and absorption (Fig. 2D).

A protein-protein interaction network was created using differentially expressed genes with an interaction score above 0.4 (Fig. 2E). Hub genes were identified using Cytoscape 2.2 with criteria: Between unDir >19, Closeness unDir >0.37, and Degree unDir >12. Detailed data is in Table 3.

3.3. Differential analysis of circRNA

Using a human circular RNA array V2.0 and a $|\log_2\text{FoldChange}| > 1$ criterion, 13,307 circRNAs were identified by comparing primary tumor tissues (T) with para-carcinoma tissue (N), revealing 1878 up-regulated and 1885 down-regulated circRNAs. In comparing liver metastasis foci (M) with T, 1875 circRNAs were up-regulated and 1634 were down-regulated (Fig. 3A). The comparison revealed 14 circRNAs that were increasingly up-regulated and 35 that were increasingly down-regulated from N to T to M (Fig. 3B and C).

3.4. Validation of circRNAs in pNET tumor tissue and liver metastases

We identified the most likely up-regulated circRNAs in pNETs tumorigenesis and metastasis by comparing fold changes in T, N, and M. Using criteria of T vs N > 1.19 and T vs M < −1.38, circRNAs has_circ_0004365, 0012779, and 0087104 were significantly up-regulated. Their source genes and sequences are detailed in Table 4. The expression levels of three up-regulated circRNAs in pNET patient samples were validated using RT-qPCR. These circRNAs showed increased expression from para-carcinoma tissue to primary tumor tissues and further to liver metastasis. However, only has_circ_0004365 exhibited significant expression differences, both between metastasis and primary tumor ($p < 0.001$) and between primary tumor and para-carcinoma tissue ($p < 0.0001$, Fig. 3D).

3.5. Construction of a circRNA-related ceRNA regulatory network and analysis of GO and KEGG pathways involving three differential circRNAs

We constructed ceRNA networks for the up-regulated circRNAs has_circ_0004365, has_circ_0012779, and has_circ_0087104 to identify potential mRNA targets (Fig. 4A–C). The networks include associated miRNA and mRNA. Using the "org.Hs.eg.db" and "clusterProfiler" R packages, we analyzed the key GO and KEGG pathways linked to these mRNAs (Fig. 5A–F).

For has_circ_0004365, a notably altered circRNA in primary tumor tissue and liver metastasis of pNET, the ceRNA-related genes were significantly involved in cellular responses to nitrogen starvation and nitrogen levels. The cell component showed enrichment in RNA polymerase II transcription regulator complex and autophagosome membrane. Molecular function was enriched in microtubule motor and exonuclease activities (Fig. 5A). The KEGG pathway for has_circ_0004365 was enriched in terpenoid backbone biosynthesis, spliceosome, apoptosis, and natural killer cell-mediated cytotoxicity (Fig. 5D).

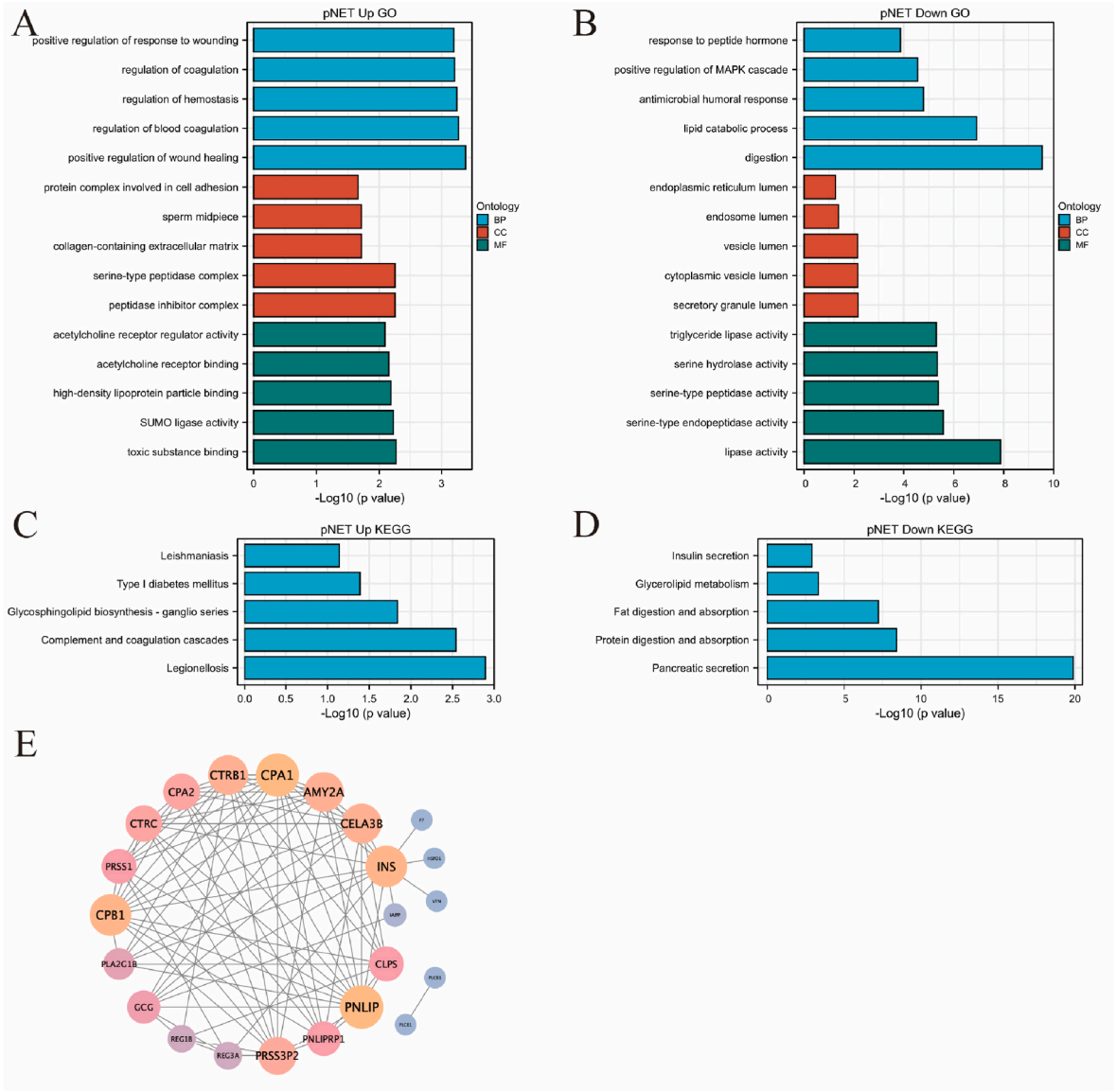

Fig. 2. Analysis of Differential Genes and Protein-Protein Interaction Network.
A. GO enrichment analysis of up-regulated pNET genes, displaying the top 5. B. GO enrichment analysis of down-regulated pNET genes, showing the top 5. C. KEGG pathway enrichment analysis for up-regulated pNET genes, highlighting the top 5 pathways. D. KEGG pathway enrichment analysis for down-regulated pNET genes, featuring the top 5 pathways. E. Protein-protein interaction network based on differentially expressed genes, using terms with *p*-values <0.05 and enrichment factors >1.5.

3.6. Analysis of intersecting GO and KEGG pathways regulated by differentially expressed circRNA-related ceRNA and mRNA

We identified seven GO pathways influenced by both differentially expressed circRNA-regulated ceRNA and mRNA. These pathways primarily involve genes related to integrin-mediated cell adhesion, integrin activation, and the biosynthesis of cellular biogenic amines, including PIEZO1, IFT74, SKAP1, GPX1, F7, VTN, and OMG (see Table 5).

3.7. Analysis of the correlation between tumor progression and gene levels of PIEZO1, IFT74, SKAP1, GPX1, F7, VTN, and OMG

RT-qPCR analysis of RNA from clinical patients revealed mRNA levels of PIEZO1, IFT74, SKAP1, GPX1, F7, VTN, and OMG. Due to sample limitations, we compared primary tumor tissue with adjacent cancer tissues (Fig. 6A), confirming significant up-regulation of SKAP1 and IFT74 in the primary cancer tissue.

3.8. Analysis of IFT74 and SKAP1 protein levels in pNETs tumor and adjacent tissues

Western blotting analysis revealed that IFT74 and SKAP1 protein levels were measured in tumor and adjacent tissues from clinical patients (Fig. 6B). SKAP1 was notably upregulated in tumor tissues ($p < 0.05$), aligning with RT-qPCR findings.

4. Discussion

pNETs are rare pancreatic tumors originating from endocrine cells, with varying malignancy. They can appear as slow-growing, non-invasive tumors, locally invasive masses, or rapidly spreading cancers [1]. Recent studies show that in sporadic pNETs, mutations in MEN1, DAXX/ATRX, and mTOR pathway genes are linked to the development and progression of pancreatic neuroendocrine tumors. Other changes involve the VEGF and Notch pathways, and germline mutations in MUTYH, CHEK2, BRCA2, PHLDA3, among other genetic alterations

Table 3
PPI implemented hub gene centralities by using 11 up-regulated and 25 down-regulated differential genes in pNET primary tumor tissue and liver metastasis foci.

Gene Name	Betweenness unDir	Betweenness Centrality	Closeness unDir	Closeness Centrality	Degree	Degree unDir
CPA1	19.81392496	0.052141908	0.038461538	0.769230769	14	14
PNLIP	19.81392496	0.052141908	0.038461538	0.769230769	14	14
INS	133.7417749	0.351952039	0.037037037	0.740740741	13	13
CPB1	14.45180375	0.038031063	0.037037037	0.740740741	13	13
AMY2A	13.62027417	0.035842827	0.035714286	0.714285714	12	12
CELA3B	12.97647908	0.034148629	0.035714286	0.714285714	12	12
CTRB1	10.20079365	0.026844194	0.03125	0.625	12	12
PRSS3P2	13.73015873	0.036131997	0.03030303	0.606060606	11	11
CTRC	7.475468975	0.019672287	0.033333333	0.666666667	10	10
CPA2	1.265873016	0.003331245	0.029411765	0.588235294	10	10
CLPS	5.341269841	0.014055973	0.028571429	0.571428571	9	9
PRSS1	4.722222222	0.012426901	0.028571429	0.571428571	9	9
PNLIPRP1	1.376984127	0.003623642	0.028571429	0.571428571	9	9
GCG	20.74393939	0.054589314	0.03125	0.625	8	8
PLA2G1B	3.03030303	0.007974482	0.03030303	0.606060606	7	7
REG3A	8.996969697	0.023676236	0.028571429	0.571428571	5	5
REG1B	4.697835498	0.012362725	0.026315789	0.526315789	5	5

[12]. Conversely, pNETs exhibit genetic changes similar to ductal adenocarcinomas, such as TP53, RB1, and KRAS mutations, along with alterations in microRNA and the immune microenvironment [13]. Advancements in genetic knowledge aid in creating management strategies for pNET patients, but the main molecules responsible for liver metastasis remain unknown. Although therapies targeting somatostatin receptors (SSTR) are safe and effective for difficult pNET cases, they primarily focus on SSTR2. Therefore, there is a pressing need for effective treatments targeting other SSTRs for patients lacking SSTR2 [14,15].

Our study identified 11 mRNA genes that were up-regulated and 25 that were down-regulated across para-carcinoma tissue, primary tumor, and metastasis sites. Enrichment analysis revealed that up-regulated genes were mainly linked to cell adhesion and coagulation pathways, while down-regulated genes were associated with enzyme activity, secretion, and metabolism in pNETs tumorigenesis and metastasis.

The down-regulation of genes related to secretion and metabolism indicates a loss of normal pancreatic function in tumor development. Our study focused on nonfunctional pNETs, excluding hormone-secreting types, using data from the GEO database. The protein-protein interaction network identified CPA1, PNLIP, INS, and CPB1 as key genes in the pNETs process. CPA1 is a carboxypeptidase that catalyzes the release of a C-terminal amino acid [16]. CPA1 mutation can lead to chronic pancreatitis in both mice and humans [17,18]. Besides, CPA1 is a highly sensitive and specific marker in acinar cell carcinoma (ACC) of the pancreas and the immunohistochemistry detection of CPA1 can benefit in diagnosing pancreatic ACC [19]. Pancreatic triacylglycerol lipase (PNLIP) is crucial for fat metabolism, breaking down long-chain fatty acid esters into 2-monoacylglycerol and free fatty acids [20]. Our study showed its down-regulation in pNETs and it also was one of the most down-regulated genes in the malignant group of primary insulinomas and metastases foci [21]. Insulin was secreted in the pancreas. Nonfunctional pNETs grow and cause organ mass effects, while functional tumors secrete hormones and are classified by the hormone type, such as insulinomas (insulin), glucagonomas (glucagon), and somatostatinomas (somatostatin). Insulinomas are the most common pNETs, often resulting in fasting hypoglycemia and hyperinsulinemia. This study used a nonfunctional pNET database from TCGA to identify new markers or treatment targets. CPB1, similar to CPA1, is a pancreatic enzyme linked to pancreatic cancer mutations [22].

Furthermore, we found that has_circ_0004365, 0012779, and 0087104 were significantly up-regulated during pNET progression and metastasis. CircRNA is a unique RNA type, typically forming a covalent closed loop through back-splicing of its 5′ and 3’ ends in animals [7]. Recent studies have indicated that circRNA is associated with many diseases [23–25]. The aberrant expression of circRNAs has been reported in many cancers through high-throughput sequencing technologies and bioinformatics [26–29]. It is found to regulate the proliferation, migration, invasion, and apoptosis of cancer cells through various mechanisms [9]. Since an early diagnosis of cancer patients is particularly critical, identifying and applying effective biomarkers are urgently required. CircRNA possesses unique properties, like great abundance, high stability, and tissue- and developmental-stage-specific expression patterns, suggesting it could serve as a potential biomarker in cancer diagnosis and prognosis [30,31]. Previous studies have validated some circRNAs promote pancreatic ductal adenocarcinoma progression through various pathways and may act as a prognostic marker or therapeutic target [32–34]. Our study confirmed the expression of has_circ_0004365, 0012779, and 0087104 in primary pNET tumors and even higher levels in liver metastases. Notably, has_circ_0004365 was significantly upregulated, suggesting its potential as a biomarker for pNET tumorigenesis and metastasis. Additionally, through ceRNA network analysis, we identified key functional enrichments in pNET, such as integrin-mediated cell adhesion regulation and FK506 binding.

To identify key mRNAs in pNET progression, we compared mRNAs from the GEO database with circRNA-ceRNA networks but found no overlap. However, we discovered commonly altered mRNAs in shared GO and KEGG pathway enrichments, specifically in GO biological processes related to integrin, cell adhesion, and their regulation. Integrins are key cell adhesion receptors for the extracellular matrix, playing a crucial role in cancer progression from tumor development to metastasis [35]. Aberrant integrin expression is confirmed in various cancers and facilitates migration and invasion [36]. In pancreatic cancer, integrin β1 enhances tumor growth, while its knockdown reduces tumor growth and prevents metastasis [37,38]. Our study suggests that the regulation of circRNA and mRNA affecting integrin activation and cell adhesion could be crucial for pNET progression and metastasis. RT-qPCR analysis of patient samples revealed significant up-regulation of SKAP1 and IFT74 in primary cancer tissues.

SKAP1, part of the src kinase family, encodes a T cell adaptor protein that recruits proteins without enzymatic activity. It regulates T cell proliferation and cell cycle progression. SKAP1 is up-regulated in colon adenocarcinoma, promoting cancer cell proliferation, invasion, and metastasis, and indicates poor prognosis in patients [39]. SKAP1 expression is positively linked to immune checkpoint molecules like PD-1, TIM-3, and LAG3 in GC tissues. Inhibiting SKAP1 may restore anti-tumor immunity and enhance immune-mediated cancer cell clearance by blocking multiple checkpoints, making SKAP1 a potential biomarker and therapeutic target for GC [40]. IFT74 is a gene coding for a core intraflagellar transporter in a complex that moves ciliary proteins along axonal microtubules. It is linked to male infertility, low sperm count, and Joubert syndrome, but not cancer, which is not discussed

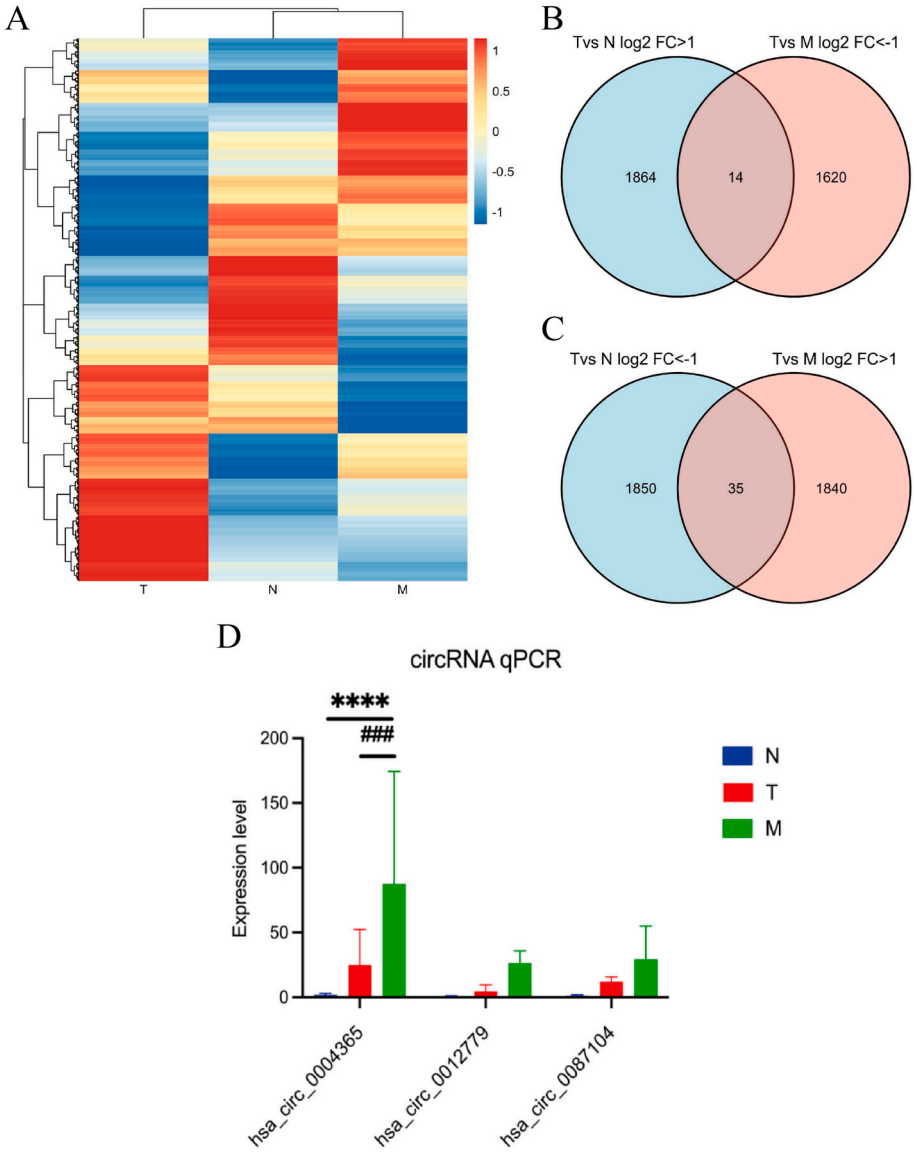

Fig. 3. Analysis of circRNA expression in pNET patients.
A. Comparison of circRNA expression in pNET primary tumors (T), liver metastases (M), and adjacent non-cancerous tissues (N). B. Identified 14 circRNAs with increased expression in T compared to N and M. C. Identified 35 circRNAs with decreased expression in T compared to N and M. D. RT-qPCR analysis of three significantly altered circRNAs: hsa_circ_0004365, hsa_circ_0012779, hsa_circ_0087104. Data are mean ± SD. Differences between two groups were assessed with Student's t-test, and ANOVA was used for multiple groups, using GraphPad Prism 8.0. Results were significant at $p < 0.05$. Significance levels: *$p < 0.05$; **$p < 0.01$; ***$p < 0.001$; ****$p < 0.0001$; ns, not significant.

Table 4
The source genes and sequences of the three changed circRNAs in pNET.

circRNA	Alias	Gene Symbol	Chrom	strand	[N](normalized)	[T](normalized)	[M](normalized)	Sequence
hsa_circRNA_100247	hsa_circ_0012779	INADL	chr1	+	5.288713802	6.483917176	7.870917178	AGATATGCCACTGATACATGGACCCTTTAGATCCTACAAGATCAGTGATTGATCCGCT
hsa_circRNA_104785	hsa_circ_0087104	CNTNAP3	chr9	–	5.783708711	7.193997958	9.255830268	ACACCTATTATTTTGGAGAATCTGAGGTGGTTTATTTTGATGGACAAAGTGCTCTGCTGT
hsa_circRNA_104421	hsa_circ_0004365	SEMA3C	chr7	–	4.828984765	6.296266944	7.836090072	GAGATACCATGTCCTGTTTCTGGGAACAGGACCAAGTTTTCATGATTGACTCCAAGTGTG

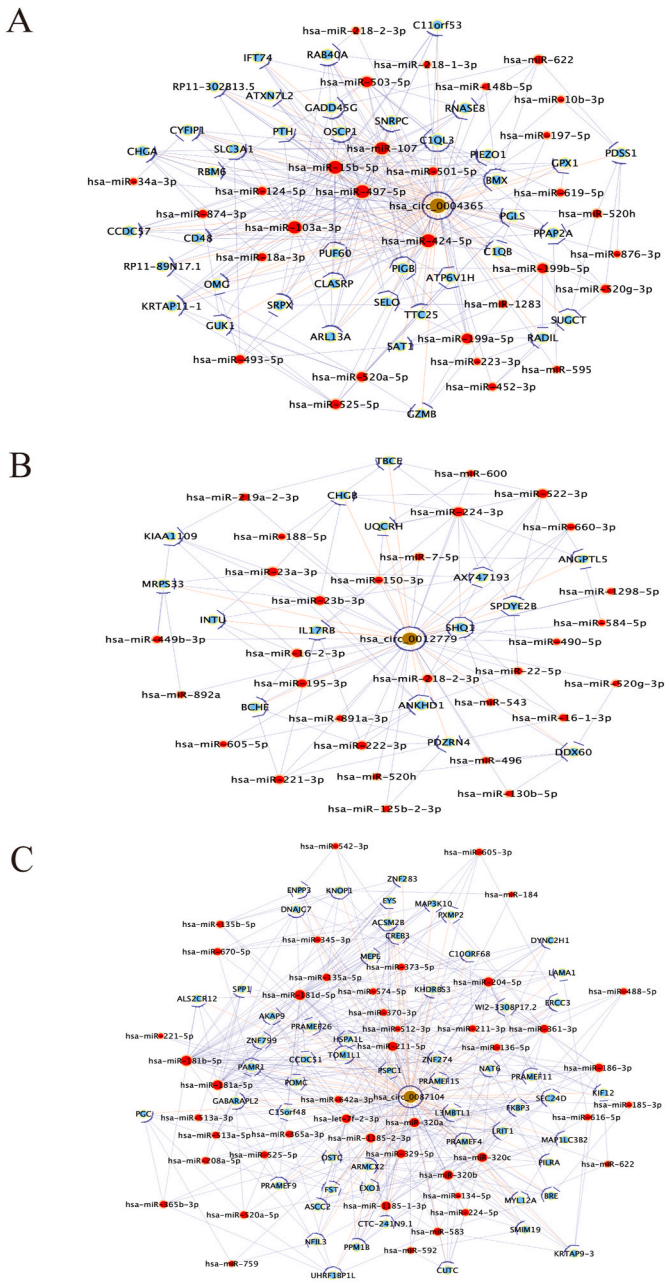

Fig. 4. Construction of the ceRNA global network using differential circRNAs
A. Network for hsa_circ_0004365; B. Network for hsa_circ_0012779; C. Network for hsa_circ_0087104. CircRNA-miRNA interactions were identified via the miRcode database, and miRNA-targeted mRNAs were predicted using miRTarBase, miRDB, and TargetScan. Only mRNAs found in all three databases were included in the network. Nodes represent enriched terms and are color-coded by RNA type: yellow for circRNA, red for miRNA, and blue for mRNA.

here [41]. To sum up, we think SKAP1 is a potential biomarker and therapeutic target for pNET.

5. Conclusion

Our findings identified 11 up-regulated and 25 down-regulated genes, along with 14 up-regulated and 35 down-regulated circRNAs, which may be crucial in pNET tumorigenesis and metastasis. Common GO and KEGG enrichment analyses of these RNAs highlighted integrin and cell adhesion pathways as key factors. SKAP1 emerges as a potential biomarker and therapeutic target for pNET.

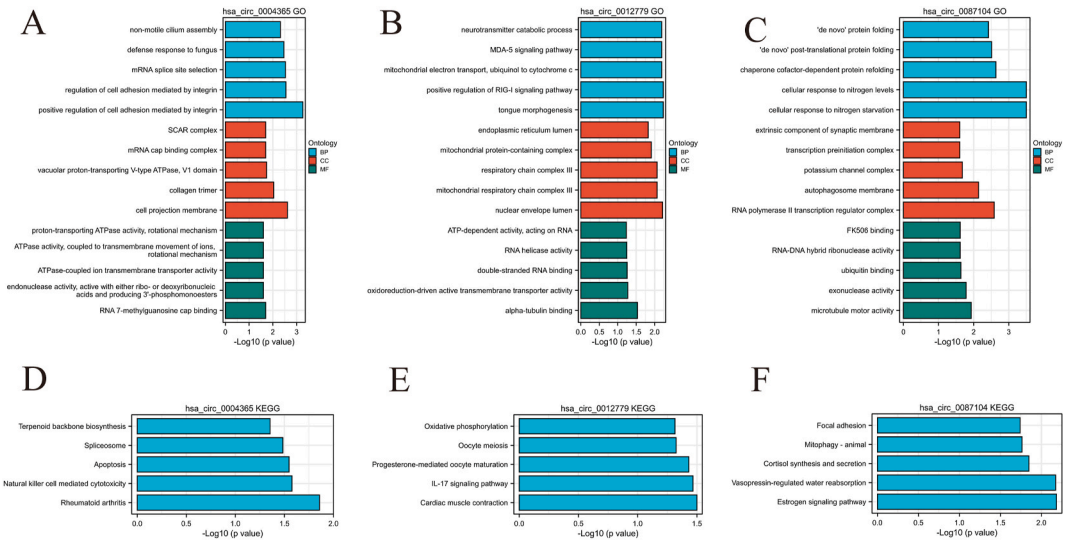

Fig. 5. Differential circRNA enrichment in pNET and KEGG analysis
A-C. Key GO enrichment analyses for hsa_circ_0004365, hsa_circ_0012779, and hsa_circ_0087104, respectively. D-F. KEGG pathway enrichment analyses for hsa_circ_0004365, hsa_circ_0012779, and hsa_circ_0087104, respectively. BP: biological process; CC: cell component; MF: molecular function.

Table 5
Intersection analysis of GO and KEGG pathways regulated commonly by different expressed circRNA-ceRNA and different expressed mRNA at the same time.

Ontology	ID	Description	Gene ID	
			Regulated by different expressed mRNA	Regulated by circRNA-ceRNA network
BP	GO:0031099	regeneration	F7/VTN	OMG/GPX1
BP	GO:0033622	integrin activation	SKAP1	PIEZO1
BP	GO:0033623	regulation of integrin activation	SKAP1	PIEZO1
BP	GO:0033627	cell adhesion mediated by integrin	VTN/SKAP1	PIEZO1/ IFT74
BP	GO:0033628	regulation of cell adhesion mediated by integrin	SKAP1	PIEZO1/ IFT74
BP	GO:0033631	cell-cell adhesion mediated by integrin	SKAP1	PIEZO1
BP	GO:0033632	regulation of cell-cell adhesion mediated by integrin	SKAP1	PIEZO1

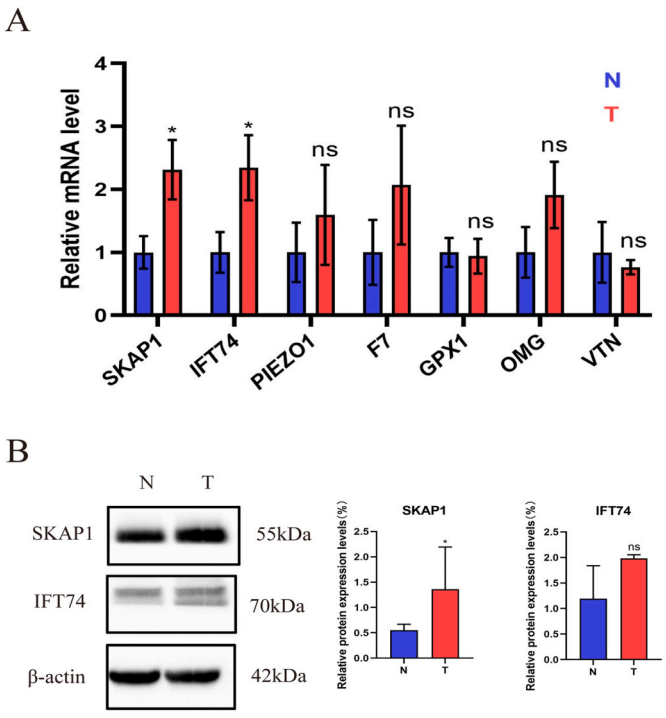

Fig. 6. Gene and protein levels in primary tumor (T) and adjacent (N) tissues
A. RT-qPCR measured mRNA levels of PIEZO1, IFT74, SKAP1, GPX1, F7, VTN, and OMG in patient samples. B. Western blot analyzed IFT74 and SKAP1 protein levels. Comparisons were made between tumor (T) and adjacent (N) tissues. Data are presented as mean ± SEM. Student's t-test and ANOVA were used for statistical analysis with GraphPad Prism 8.0. Results are significant if $p < 0.05$; * indicates $p < 0.05$, ns indicates no significance.

CRediT authorship contribution statement

Gang Li: Writing – original draft, Data curation. **Jing Zhang:** Writing – review & editing, Writing – original draft, Data curation. **Bentuo Zhang:** Data curation. **Dan Wang:** Data curation. **Zequn Wang:** Data curation. **Yan Pan:** Writing – review & editing, Supervision. **Lijie Ma:** Writing – review & editing, Supervision.

Ethics approval and consent to participate

The Peking University Third Hospital Ethics Committee approved this study, and all patients provided written consent before tissue sample collection.

Consent for publication

Not applicable.

Availability of data and materials

All data generated or analyzed during this study are included in this article.

Funding

Supported by the National Natural Science Foundation of China (Grant No. 82473947).

Declaration of competing interest

The authors hereby declare that there are no conflicts of interest associated with this publication.

Abbreviations

PNET	Primary pancreatic neuroendocrine tumor
CircRNA	Circular RNA
CeRNA	competitive endogenous RNA
RBPs	RNA binding proteins
DEGs	differentially expressed genes

Appendix A. Supplementary data

Supplementary data to this article can be found online at https://doi.org/10.1016/j.bbrep.2025.101935.

Data availability

Data will be made available on request.

References

[1] G. Perri, L.R. Prakash, M.H.G. Katz, Pancreatic neuroendocrine tumors, Curr. Opin. Gastroenterol. 35 (5) (2019) 468–477.
[2] C.K. Maharjan, et al., Pancreatic neuroendocrine tumors: molecular mechanisms and therapeutic targets, Cancers 13 (20) (2021).
[3] M. Cives, J.R. Strosberg, Gastroenteropancreatic neuroendocrine tumors, Ca - Cancer J. Clin. 68 (6) (2018) 471–487.
[4] M.B. Sonbol, et al., Survival and incidence patterns of pancreatic neuroendocrine tumors over the last 2 decades: a seer database analysis, Oncol. 27 (7) (2022) 573–578.
[5] A. Akirov, et al., Treatment options for pancreatic neuroendocrine tumors, Cancers 11 (6) (2019).
[6] X. Yang, et al., High-throughput transcriptome profiling in drug and biomarker discovery, Front. Genet. 11 (2020) 19.
[7] L.S. Kristensen, et al., The biogenesis, biology and characterization of circular RNAs, Nat. Rev. Genet. 20 (11) (2019) 675–691.
[8] H. Wang, et al., Circular RNAs regulate parental gene expression: a new direction for molecular oncology research, Front. Oncol. 12 (2022) 947775.
[9] L. Chen, G. Shan, CircRNA in cancer: fundamental mechanism and clinical potential, Cancer Lett. 505 (2021) 49–57.
[10] M. Kanehisa, et al., KEGG: integrating viruses and cellular organisms, Nucleic Acids Res. 49 (D1) (2021) D545–d551.
[11] Z.D. Yang, H. Kang, Exploring prognostic potential of long noncoding RNAs in colorectal cancer based on a competing endogenous RNA network, World J. Gastroenterol. 26 (12) (2020) 1298–1316.
[12] H. Ishida, A.K. Lam, Pancreatic neuroendocrine neoplasms: updates on genomic changes in inherited tumour syndromes and sporadic tumours based on WHO classification, Crit. Rev. Oncol. Hematol. 172 (2022) 103648.
[13] E.S.A. Egal, et al., Translational challenges in pancreatic neuroendocrine tumor immunotherapy, Biochim. Biophys. Acta Rev. Canc 1876 (2) (2021) 188640.
[14] Y. Hu, et al., Role of somatostatin receptor in pancreatic neuroendocrine tumor development, diagnosis, and therapy, Front. Endocrinol. 12 (2021) 679000.
[15] A. Chang, et al., Progress in the management of pancreatic neuroendocrine tumors, Annu. Rev. Med. 73 (2022) 213–229.
[16] R.M. Laethem, et al., Expression and characterization of human pancreatic preprocarboxypeptidase A1 and preprocarboxypeptidase A2, Arch. Biochem. Biophys. 332 (1) (1996) 8–18.
[17] E. Hegyi, M. Sahin-Tóth, Human CPA1 mutation causes digestive enzyme misfolding and chronic pancreatitis in mice, Gut 68 (2) (2019) 301–312.
[18] M. Sándor, et al., Novel p.G250A mutation associated with chronic pancreatitis highlights misfolding-prone region in carboxypeptidase A1 (CPA1), Int. J. Mol. Sci. 23 (24) (2022).
[19] R. Uhlig, et al., Carboxypeptidase A1 (CPA1) immunohistochemistry is highly sensitive and specific for acinar cell carcinoma (ACC) of the pancreas, Am. J. Surg. Pathol. 46 (1) (2022) 97–104.
[20] A.M. van Bennekum, et al., Hydrolysis of retinyl esters by pancreatic triglyceride lipase, Biochemistry 39 (16) (2000) 4900–4906.
[21] F.O. Buishand, et al., Gene expression profiling of primary canine insulinomas and their metastases, Vet. J. 197 (2) (2013) 192–197.
[22] K. Tamura, J. Yu, T. Hata, M. Suenaga, K. Shindo, T. Abe, A. MacGregor-Das, M. Borges, C.L. Wolfgang, M.J. Weiss, J. He, M.I. Canto, G.M. Petersen, S. Gallinger, S. Syngal, R.E. Brand, A. Rustgi, S.H. Olson, E. Stoffel, M.L. Cote, G. Zogopoulos, J.B. Potash, F.S. Goes, R.W. McCombie, P.P. Zandi, M. Pirooznia, M. Kramer, J. Parla, J.R. Eshleman, N.J. Roberts, R.H. Hruban, A.P. Klein, M. Goggins, Mutations in the pancreatic secretory enzymes CPA1 and CPB1 are associated with pancreatic cancer, Proc. Natl. Acad. Sci. U. S. A. 115 (18) (2018 May 1) 4767–4772.
[23] M.A. Altesha, et al., Circular RNA in cardiovascular disease, J. Cell. Physiol. 234 (5) (2019) 5588–5600.
[24] A.J. van Zonneveld, et al., Circular RNAs in kidney disease and cancer, Nat. Rev. Nephrol. 17 (12) (2021) 814–826.
[25] Y. Wang, et al., Exosomal circRNAs: biogenesis, effect and application in human diseases, Mol. Cancer 18 (1) (2019) 116.
[26] R. Li, et al., CircRNA: a rising star in gastric cancer, Cell. Mol. Life Sci. 77 (9) (2020) 1661–1680.
[27] G. Zhu, et al., A novel potential strategy to treat thyroid cancer (Review), Int. J. Mol. Med. 48 (5) (2021 Nov) 201.
[28] M. Zhang, et al., circRNA-miRNA-mRNA in breast cancer, Clin. Chim. Acta 523 (2021) 120–130.
[29] X. Yang, et al., Expression profiles, biological functions and clinical significance of circRNAs in bladder cancer, Mol. Cancer 20 (1) (2021) 4.
[30] H.D. Zhang, et al., CircRNA: a novel type of biomarker for cancer, Breast Cancer 25 (1) (2018) 1–7.
[31] L. Chen, et al., The bioinformatics toolbox for circRNA discovery and analysis, Briefings Bioinf. 22 (2) (2021) 1706–1728.
[32] C.H. Wong, et al., CircRTN4 promotes pancreatic cancer progression through a novel CircRNA-miRNA-lncRNA pathway and stabilizing epithelial-mesenchymal transition protein, Mol. Cancer 21 (1) (2022) 10.
[33] C.H. Wong, et al., CircFOXK2 promotes growth and metastasis of pancreatic ductal adenocarcinoma by complexing with RNA-binding proteins and sponging MiR-942, Cancer Res. 80 (11) (2020) 2138–2149.
[34] P. Shen, et al., CircNEIL3 regulatory loop promotes pancreatic ductal adenocarcinoma progression via miRNA sponging and A-to-I RNA-editing, Mol. Cancer 20 (1) (2021) 51.
[35] H. Hamidi, J. Ivaska, Every step of the way: integrins in cancer progression and metastasis, Nat. Rev. Cancer 18 (9) (2018) 533–548.
[36] L. Bao, et al., The human ion channel TRPM2 modulates migration and invasion in neuroblastoma through regulation of integrin expression, Sci. Rep. 12 (1) (2022) 20544.
[37] M.S. Mia, et al., Integrin β1 promotes pancreatic tumor growth by upregulating kindlin-2 and TGF-β receptor-2, Int. J. Mol. Sci. 22 (19) (2021).
[38] J.J. Grzesiak, et al., Knockdown of the β(1) integrin subunit reduces primary tumor growth and inhibits pancreatic cancer metastasis, Int. J. Cancer 129 (12) (2011) 2905–2915.
[39] Y. Pu, et al., THUMPD3-AS1 facilitates cell growth and aggressiveness by the miR-218-5p/SKAP1 axis in colorectal cancer, Cell Biochem. Biophys. 82 (1) (2024) 315.
[40] L. Zhu, et al., SKAP1 is a novel biomarker and therapeutic target for gastric cancer: evidence from expression, functional, and bioinformatic analyses, Int. J. Mol. Sci. 24 (14) (2023) 11870.
[41] M. Luo, et al., Disrupted intraflagellar transport due to IFT74 variants causes Joubert syndrome, Genet. Med. 23 (6) (2021 Jun) 1041–1049.